Substrate specificity of the FurE transporter is determined by cytoplasmic terminal domain interactions

Georgia F. Papadaki, Sotiris Amillis, and George Diallinas

Supplemental Material

Table S1. Oligonucleotides used in this study.

Oligonucleotide	5'-3' Sequence
GFP NotI R	CGC**GCGGCCGC**TTACTTGTACAGCTCGTCC
GFP PstI R	AA**CTGCAG**TTACTTGTACAGCTCGTCCATGC
FurD SpeI F	GCG**ACTAGT**ATGCGTTTCGGTCGCTTTCACC
FurA SpeI F	GCG**ACTAGT**ATGTCAGCTATTAAACGATGGATC
FurC SpeI F	GCG**ACTAGT**ATGGACCGCCTCTCCATCAG
FurE SpeI F	GCG**ACTAGT**ATGGGACTACGAGAAAGACTCC
FurA K534 NS NotI R	GCG**GCGGCCGC**GCCGGTGTGGATATCTTCCG
FurD K531 NS NotI R	GCG**GCGGCCGC**GCTCTCCCCCAACTCCTCCC
FurE K498 NS NotI R	GCG**GCGGCCGC**CTCTTCAACATCAAACGGCCAG
gpdA (1000) AatII F	GCG**GACGTC**GGTTGACCGGTGCCTGGATC
YFPn XbaI F2	CGCG**TCTAGA**ATGGTGAGCAAGGGCGAGGAGCTG
YFPn SpeI R	CGCG**ACTAGT**TTACATGATATAGACGTTGTGGCTGTTG
YFPc BamHI F	CGCG**GGATCC**ATGGCCGACAAGCAGAAGAAC
YFPc NS BamHI R	CGCG**GGATCC**CTTGTACAGCTCGTCCATG
YFPn BamHI F	CGCG**GGATCC**ATGGTGAGCAAGGGCGAGGAGCTG
YFPn NS BamHI R	CGCG**GGATCC**CATGATATAGACGTTGTGGCTGTTG
FurD BglII F	GCCG**AGATCT**ATGCGTTTCGGTCGCTTTCACC
FurD XbaI NS R	GCGC**TCTAGA**TAAACAGCAAAACCCTTCTCC
FurE BamHI F	GCCG**GGATCC**ATGGGACTACGAGAAAGACTCC
FurE XbaI NS R	GCGC**TCTAGA**GCAGAGACAGCCTCCTTCTTCTGCACC
FurEN21 SpeI F	CGCG**ACTAGT**ATGGCCTCCAACAAAGACCTCG
GFP NotI dstr F	GACGAGCTGTACAAGTAAGCGAACGCGATCCACTTAACGTTACTG
GFP NotI dstr R	CAGTAACGTTAAGTGGATCGCGTTCGCTTACTTGTACAGCTCGTC
FurE K498 XbaI R	GCG**TCTAGA**CTACTCTTCAACATCAAACGGCCAGAC
gpdA NotI F	GCG**GCGGCCGC**GCATGCCATTAACCTAGGTACAGAAGTCC
FurE Y392N F	GCTTTTCATCTTTTCTAGGTGGGAACAGCCTGTTTCTTGGTGC
FurE Y392N R	GCACCAAGAAACAGGCTGTTCCCACCTAGAAAAGATGAAAAGC
FurE T133V F	CGCTATTATCTGGTTTGGCGTGCAGACGTACCAGGCCG
FurE T133V R	CGGCCTGGTACGTCTGCACGCCAAACCAGATAATAGCG
FurE seq 1	CGCCGTCTTCGGTATGCTTCC
FurE seq 2	CGCGGTACGCCAAAACTCCCAG

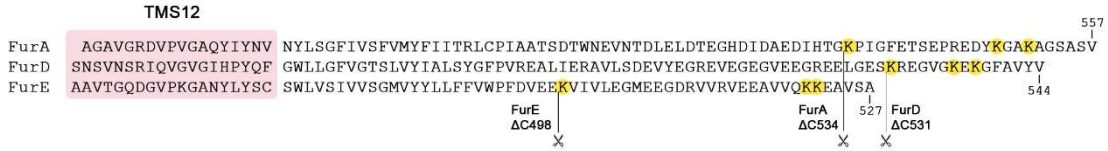

Figure S1. Alignment of the C-terminal regions of FurA, FurD and FurE transporters. Positions of truncations and potential ubiquitin acceptor Lys residues are highlighted. The last transmembrane domain, TMS12, is also highlighted.

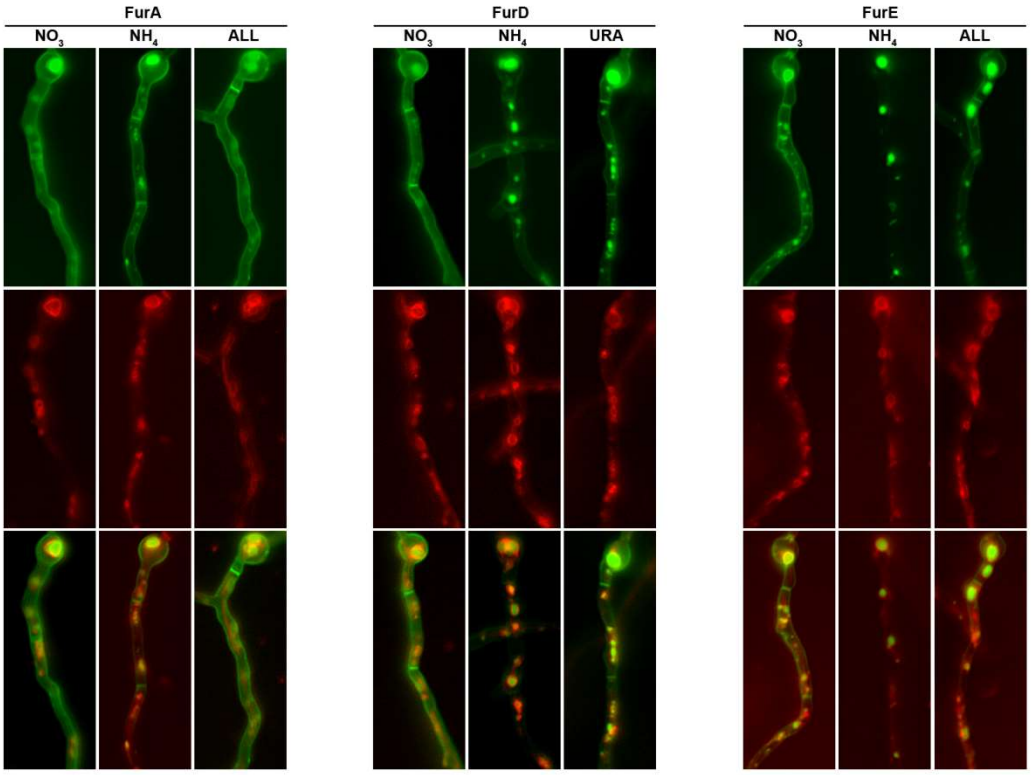

Figure S2. Epifluorescence microscopy showing the nearly absolute co-localization of GFP fluorescent signal, coming from degradation of the Fur-GFP chimaeras, with the endosome/vacuole-specific FM4-64 molecular stain. Conditions for strain growth and microscopic analysis are as described in Materials and methods. Conditions for vacuolar staining with FM4-64 are as described in Martzoukou *et al*. 2017.

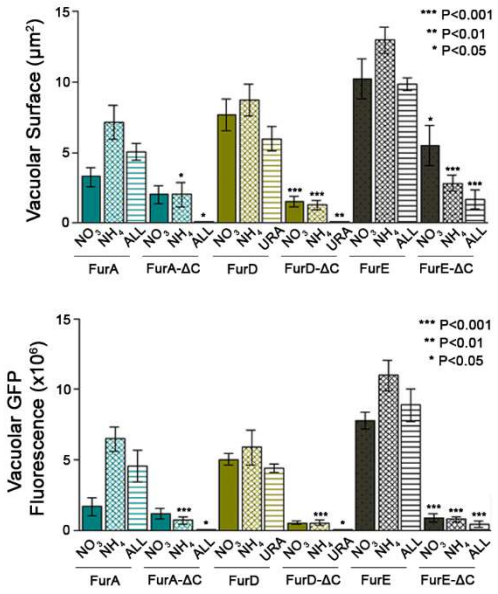

Figure S3. Quantification and statistical analyses of endocytosis, as measured by estimating the surface and intensity of vacuolar GFP fluorescence. Standard deviation is depicted with error bars (n=5) (see Materials and Methods).

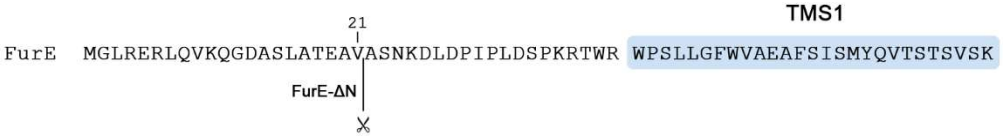

Figure S4. N-terminal region of FurE showing the truncated segment in FurE-ΔN. The first transmembrane domain, TMS1, is also highlighted.

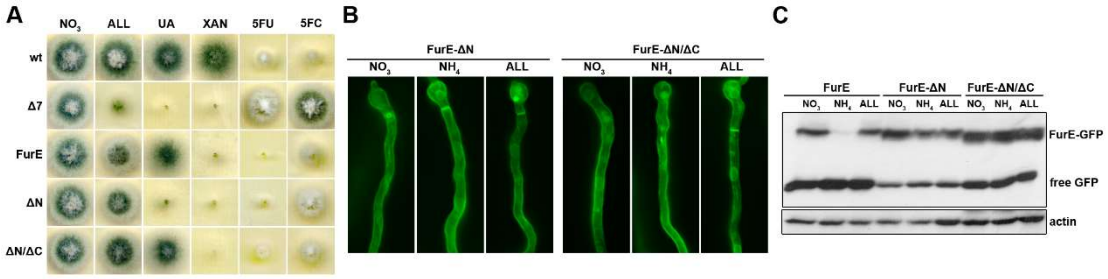

Figure S5. Functional analysis of doubly truncated FurE-ΔN/ΔC. (**A**) Growth tests of mutants and control strains (WT, Δ7, FurE and ΔN) in MM containing nitrate (control), uric acid (UA), allantoin (ALL) or xanthine (Xan) as N sources, or on nitrate media containing 5-fluorouracil (5FU) or 5-fluorocytosine (5FC). All growth tests shown were performed at 37ºC. (**B**) Subcellular localization of FurE-ΔN and FurE-ΔN/ΔC mutants analyzed by *in vivo* epifluorescence microscopy. (**C**) Protein steady state levels of FurE, FurE-ΔN and FurE-ΔN/ΔC, detected by western blot analysis using anti-GFP (upper panel) or anti-actin (control, lower panel) antibodies, as described in Materials and methods (the blot concerning FurE is the same as that shown in Figure 3D, left panel).